HYDROLOGICAL PROCESSES
Hydrol. Process. (2011)
Published online in Wiley Online Library
(wileyonlinelibrary.com) DOI: 10.1002/hyp.8329

Snow measurement by GPS interferometric reflectometry: an evaluation at Niwot Ridge, Colorado

Ethan D. Gutmann,[1]* Kristine M. Larson,[2] Mark W. Williams,[3] Felipe G. Nievinski[2] and Valery Zavorotny[4]

[1] *Research Applications Lab, National Center for Atmospheric Research, Boulder, CO, USA*
[2] *Department of Aerospace Engineering Sciences, University of Colorado, Boulder, CO, USA*
[3] *Department of Geography and INSTAAR, University of Colorado, Boulder, CO, USA*
[4] *Earth Systems Research Laboratory, NOAA, Boulder, CO, USA*

Abstract:

Snow is a critical storage component in the hydrologic cycle, but current measurement networks are sparse. In addition, the heterogeneity of snow requires surveying larger areas to measure the areal average. We presented snow measurements using GPS interferometric reflectometry (GPS-IR). GPS-IR measures a large area (~100 m^2), and existing GPS installations around the world have the potential to expand existing snow measurement networks. GPS-IR uses a standard, geodetic GPS installation to measure the snow surface via the reflected component of the signal. We reported GPS-IR snow depth measurements made at Niwot Ridge, Colorado, from October 2009 through June 2010. This site is in a topographic saddle at 3500 m elevation with a peak snow depth of 1.7 m near the GPS antenna. GPS-IR measurements are compared with biweekly snow surveys, a continuously operating scanning laser system and an airborne light detection and ranging (LIDAR) measurement. The GPS-IR measurement of peak snowpack (1.36–1.76 m) matches manual measurements (0.95–1.7 m) and the scanning laser (1.16 m). GPS-IR has RMS error of 13 cm (bias = 10 cm) compared with the laser, although differences between the measurement locations make comparison imprecise. Over the melt season, when the snowpack is more homogenous, the difference between the GPS-IR and the laser is reduced (RMS = 9 cm, bias = 6 cm). In other locations, the GPS and the LIDAR agree on which areas have more or less snow, but the GPS estimates more snow on the ground on tracks to the west (1.58 m) than the LIDAR (1.14 m). Copyright © 2011 John Wiley & Sons, Ltd.

KEY WORDS GPS; snow; measurement technique; Niwot Ridge; GPS-IR; remote sensing

Received 14 February 2011; Accepted 15 September 2011

INTRODUCTION

Snow is an important water resource with many economic, residential and ecosystem uses. Indeed, more than one-sixth of the world's population lives in river basins fed by snow or glacier melt. As a result, glacial retreat or decreased snow water storage is likely to adversely affect human and ecosystem functioning, particularly in semiarid regions (Barnett *et al*., 2005; Parry *et al*., 2007). These changes in frozen water storage can affect seasonal shifts in stream flow and reduce low flows. Snow is also the basis for the multibillion dollar per year ski industry, and snowmobiling alone brings in more than $27 billion dollars annually in North America (Scott *et al*., 2008).

Despite its importance, measurement of snow is difficult because of its high spatial and temporal variability (Erickson *et al*., 2005; Armstrong and Brun, 2008). Current ground-based measurement techniques include manual and automated ones, each with their own benefits and limitations (Eisen *et al*., 2008). Manual measurements include snow sticks for surveying snow depth and snow density measurements with a device such as a federal sampler. However, manual measurements miss temporal dynamics of accumulation and ablation because the manual labour involved is costly; thus, these measurements are infrequently carried out (commonly once or twice per month; e.g. Litaor *et al*., 2008). Furthermore, on a global scale, their value is often reduced by large inconsistencies in methods, frequency and standards (IGOS, 2007). Current automated measurements include sonic depth measurement, snow pillows and gamma radiation measurement. These automated methods have higher temporal resolution but miss important spatial variability because of their limited spatial footprints. In contrast, new automated methods do have a larger footprint, such as cosmic ray neutron measurements (Desilets *et al*., 2010) (~0.5–1 km^2 footprint), but even it is a spatially averaged measurement. Ground-based radars (Hardy *et al*., 2008) and terrestrial laser scanners (Prokop, 2008) improve our knowledge of the spatial distribution of snow by resolving its spatial variability but often lack the temporal coverage. In addition, spatially averaged estimates from intermediate-scale sensors are preferable to point-scale *in situ* probes for the validation of airborne and space-borne remote sensing instruments (ESA, 2008).

*Correspondence to: Ethan Gutmann, Research Applications Lab, National Center for Atmospheric Research, Boulder, CO, USA.
E-mail: gutmann@ucar.edu

A promising new method for the automated measurement of snow properties is GPS interferometric reflectometry (GPS-IR) (Larson *et al*., 2009). This method is essentially an L-band ground-based interferometer. Its working principle is the interference between direct or line-of-sight signal and multipath signals, reflected off near-ground surfaces (snow, bare soil, etc.). GPS-IR uses signals from the constellation of 30+ GPS satellites and existing GPS stations. Although the GPS ground stations were initially deployed and are currently maintained for geophysical and surveying applications, it has been shown that these geodetic-quality receivers are capable of ground-based remote sensing. Larson *et al*. (2008) was the first to demonstrate that GPS signal power measured by geodetic-quality GPS receivers correlates with changes in soil moisture, which was followed by additional studies that demonstrated strong correlations with snow depth (Larson *et al*., 2009) and vegetation (Small *et al*., 2010).

This initial work showed that GPS-IR can measure snow depth (Larson *et al*., 2009) in a topographically flat and nearly horizontal site (tilt $< 1°$) during two discrete snow events. More recent work has shown that it may be possible to estimate snow water equivalent (SWE) from GPS reflections (Jacobson, 2008, 2010). Here, we present new results from a GPS unit installed at 3500 m on Niwot Ridge in Colorado through the winter of 2010. This site is substantially more complex both topographically and environmentally than previous studies, with a relatively complex snow stratigraphy. We first describe the general principles behind GPS-IR, followed by a description of the site, the GPS installation at Niwot Ridge and its use to derive snow depth. This is followed by a description of the data sets used for verification. Finally, we present comparisons between GPS-IR-derived snow depth and manual observations of snow depth and density as well as snow depth from a co-located scanning laser rangefinder and an airborne light detection and ranging (LIDAR) survey.

GPS REFLECTIONS

For most of its history, GPS satellites have transmitted two coded signals at L-band frequencies. The primary frequency (L1) is at 1.57542 GHz and the secondary (L2) frequency is at 1.2276 GHz. These frequencies correspond to wavelengths of ~ 19.0 and 24.4 cm. Large networks of continuously operating geodetic-quality receivers track these GPS signals. Some of these networks were installed to help surveyors (e.g. Continuously Operating Reference Station, http://www.ngs.noaa.gov/CORS/); others were installed by geoscientists wishing to measure small (1–100 mm/year) ground motions related to plate tectonics [e.g. EarthScope Plate Boundary Observatory (PBO), see http://pboweb.unavco.org] as well as larger episodic displacements associated with earthquakes. Although positioning applications only use GPS ranging observations, most of these networks record (and archive) GPS signal power too [in the form of signal-to-noise ratio (SNR)], which is the observable used in GPS-IR. Although we tracked all satellites in the GPS constellation at Niwot, we will only interpret a subset of the satellites for snow sensing. In particular, we only used data from satellites that transmit a new civilian code made available on the L2 carrier frequency (Fontana *et al*., 2001). This includes all satellites launched from 2005 to present (PRN numbers 5, 7, 12, 15, 17, 29 and 31), with the exception of PRN 1, which has been set as permanently unhealthy by the Department of Defense. The signal power data quality for L2 carrier frequency is superior to the other signals on the Trimble NetRS receiver (Larson *et al*., 2010). The gain pattern of a geodetic-quality GPS antenna is designed to suppress reflections. However, fortunately for the application studied here, the reflections are not completely suppressed, and the lowest elevation angle data ($5°$–$30°$) can typically be used for snow sensing.

NIWOT RIDGE SITE

The study was conducted at the Niwot Ridge saddle (3500 m elevation), located in the Colorado Front Range of the Rocky Mountains, approximately 5 km east of the Continental Divide (40º 03′N, 105º 35′W). The saddle site is a north–south-oriented trough that becomes progressively steeper to the east and west. Within the saddle, a research grid 550 m long and 400 m wide was established in the late 1980s, marked by 88 poles on 50-m centres (Litaor *et al*., 2008). Niwot Ridge is a broad interfluve and is characterised by low rounded hills with shallow saddles in between (Figure 1). This site is a United Nations Educational, Scientific and Cultural Organization Biosphere Reserve and a Long-Term Ecological Research (LTER) network site. The climate is characterised by long, cool winters and a short growing season (1–3 months). Since 1951, the mean annual temperature is $-3.8\,°C$ and the annual precipitation is around 1000 mm, recorded at meteorological station D1 located above the saddle site (Williams *et al*., 1996). Approximately 80% of annual precipitation falls as snow (Caine, 1996) and is redistributed by westerly winds (mean direction 255º to 275º, average velocity of 10–13 m/s; Erickson *et al*., 2005), causing snow depth on the saddle to vary by a factor of ten or more, depending on terrain factors. Vegetation is alpine tundra, which is perennial, low in stature and easily covered by accumulating snow. Thus, surface roughness is relatively homogeneous over the study area, with maximum snow depths of greater than 5 m, more than 10 times greater than the maximum heights of herbaceous vegetation of approximately 0.2 m (Litaor *et al*., 2008). Meteorological measurements sufficient to close the energy balance and parameterise energy-balance snowmelt models are made 50 m to the south-southeast of pole 6 (Williams *et al*., 1999).

GPS installation

The GPS site at Niwot Ridge has many similarities with other continuously operating GPS sites. For example, the same Trimble NetRS receiver used in the 1100 PBO stations was used at Niwot. This receiver can track up to 12 GPS satellites at a time on both frequencies. However,

DOI: 10.1002/hyp

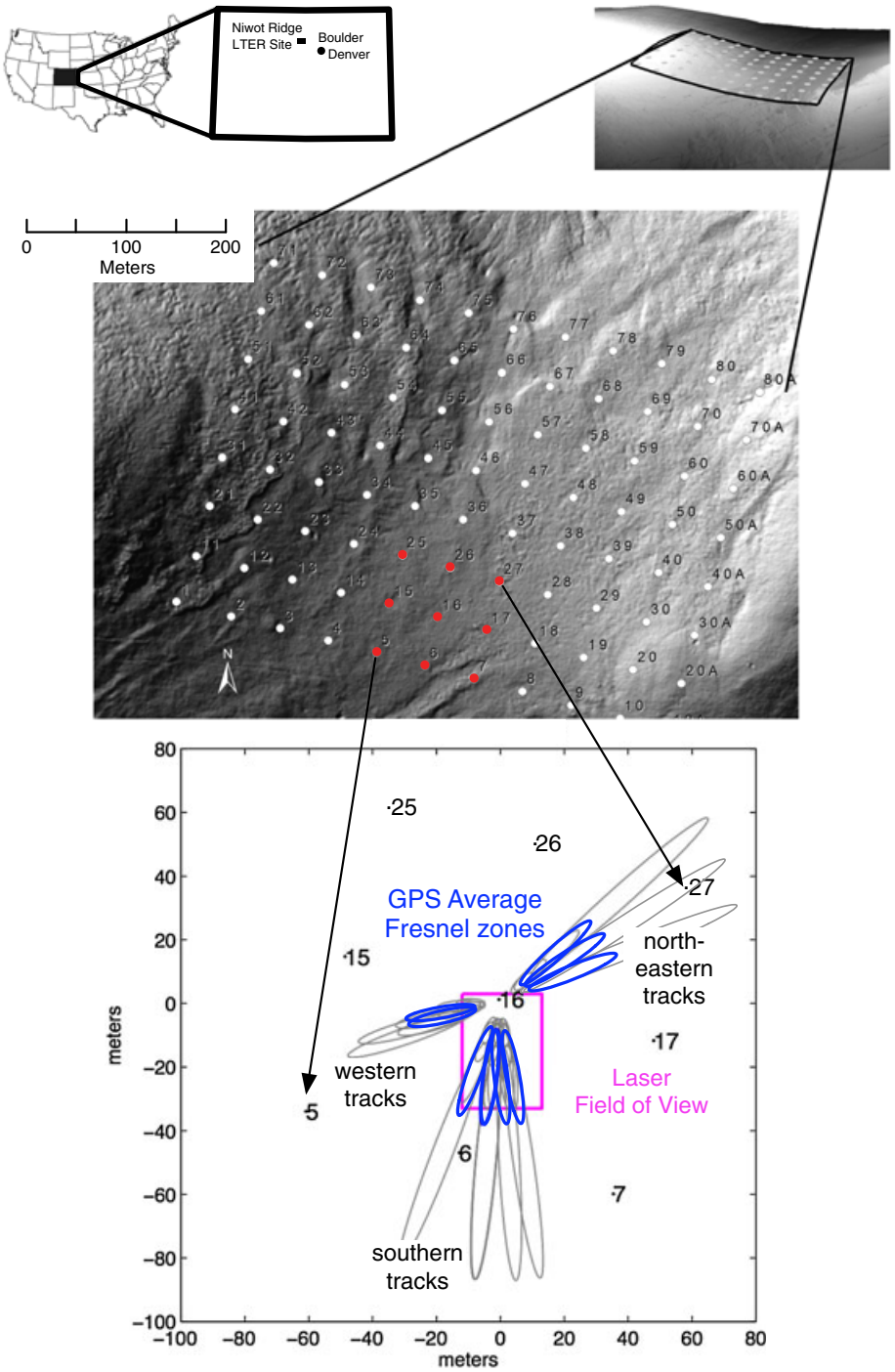

Figure 1. Site overview map with a Niwot Ridge in the state of Colorado in the upper left, a 1-m DEM (upper right) and hillshade image (centre) showing the surrounding topography, and the GPS footprints for satellite tracks (bottom) are each shown at four separate elevation angles 5°, 10°, 15° and 20°, with an average across elevation angles in blue. The laser grid is outlined in magenta, and manual pole depth measurements are labelled with numbers; red poles are those present on the inset map

the antenna setup preferred by PBO was not used. For PBO, the GPS antenna is usually anchored to the ground using steel piping—and the antenna is approximately 2 m above the ground. To be sure that the GPS would always be above snow levels at Niwot, we anchored the antenna 3 m above the ground (Figure 2). Typically, PBO covers their antennas with an acrylic radome to protect it from snow accumulation, animals nesting and vandals. A radome was not used at Niwot because strong winds at this location make it less likely that snow would accumulate on the antenna. Previous work has used an antenna with a radome on it with no noticeable difference (Larson *et al.*, 2009). The GPS was installed approximately 400 m downwind of a 100-m high rise on the ridge (Figure 1), resulting in an accumulation of snow at the site, although some of the surrounding area remains wind scoured all winter.

Most of the useful ground tracks at Niwot are to the south. For a site at 40° north latitude, there are no tracks between ±25° of north. This is because of the 55°

DOI: 10.1002/hyp

Figure 2. View south-southeast past the GPS installation at Niwot Ridge. The 3-m tall GPS is in the foreground (centre left) along with pole 16. The 5.5-m tall scanning laser is on the left with a person for scale. Sastrugi were not uncommon at the site but are not always present

inclination of the GPS satellite orbits with respect to the equator. This sky coverage void is latitude dependent, being most pronounced at mid-latitudes; for example, at the geographical poles, satellites are visible from every azimuth; in the southern hemisphere, at -40° latitude, there would be no tracks $\pm 25^\circ$ of the south azimuth. The tracks to the west and east of the GPS site at Niwot can—in principle—be used but are complicated for this site because of the local topography. Topographic rises in the east and west partially obstruct the GPS signal, significantly reducing the amount of data that can be collected as well as complicating the interpretation of the unobstructed portion. In this study, results are shown for three regions where the ground is tilted, but still mostly planar: directly to the south (5 satellite tracks), to the west (2 tracks at an azimuth of ~250°) and three tracks to the northeast (Figure 1).

Derivation of snow depth from GPS signal power data

For a planar and horizontal reflector (ground, snow, etc.), the interference between the reflected and the direct GPS signals produces approximately a sinusoid of constant frequency in SNR observations (Larson *et al.*, 2008). Multiple cycles of this modulation pattern must be observed to estimate that frequency, which is then related to the height of the antenna above the reflecting surface. Because GPS signals reflect off the snow surface, the frequency decreases with increasing snow depth. In our previous snow study (Larson *et al.*, 2009), all data between elevation angles of 5° and 30° were used. However, at Niwot, the reflected signals above elevation angles of 20° often exhibit an attenuated amplitude (Figure 3). This is mostly due to a decrease in power of the reflected signal, which is caused primarily by the antenna gain pattern. Although this example primarily shows low signal power data in the summer plot, it is also sometimes present during the winter when snow is on the ground. To have common sampling throughout the entire period for this study, we used data between 5° and 20° only. Figure 3 clearly shows changes in signal power frequency for 4 days: deep snow [day-of-year (DOY) 125 and 140], shallow snow (DOY 155) and no snow (DOY 260). It is this change in frequency that we used to infer snow depth.

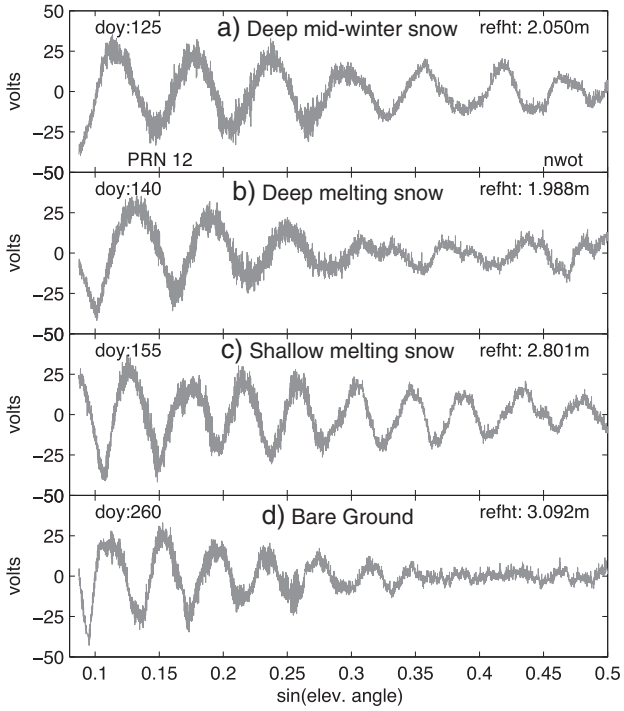

Figure 3. GPS SNR at Niwot after detrending. (a, top) Low-frequency SNR oscillations when the snow is closer to the antenna (deeper) with a lower density, dry snowpack. (b) Same as panel a but with a denser, melting snowpack. (c) High-frequency SNR oscillations when the snow is further from the antenna (shallower. (d) Higher frequency SNR oscillations over bare ground and substantially decreased amplitude at higher elevation angles. Apparent height of the antenna above the reflecting surface (refht) is listed for each panel along with the day of the year (DOY)

DOI: 10.1002/hyp

Our ultimate goal is to estimate SWE directly from GPS-IR, but in this study, only snow depth is estimated. Figure 4 shows forward model predictions for two characteristic snow density values (equivalent to the conditions at Niwot Ridge in April and May) for each of two different snow depths. The model permittivities used were as follows: for the less dense, dry snow, real = 1.68, imaginary = 3.8E−4, and for the denser snow, real = 2.178, imaginary = 8.7E−4, consistent with observations of Mätzler (1996). It is clear that there is very little difference between the two density solutions for elevation angles between the 5° and 20° elevation angles used here. Most of the difference between the solutions is seen in the signal amplitude, which is not used in our data analysis currently. The use of the amplitude data is complicated by the fact that it is also affected by the roughness of the surface, which would be expected to vary as the snow surface is scoured by wind.

The uniformity in the forward model with varying snow densities confirms that the dominant reflector is the snow–atmosphere interface; the primary changes expected from variations in density are related to the portion of the signal that is transmitted through the snow and reflected off the ground. This means that the method used here is primarily sensitive to snow depth. A 25-day dry period during the summer was used to determine the height of the antenna above bare ground. For the bare soil reflections, a correction must be made to take into account the signal penetration into the soil. A 5-cm soil penetration depth was removed from the summer Niwot data, which is consistent with what has been observed at other dry soil sites (Larson *et al*., 2010). In the winter, penetration into frozen ground is likely to be deeper, but because the dominant reflection is from the snow–air interface, this does not affect our measurement significantly.

We reported average snow depth values for the three northeastern, two western and five southern tracks and a standard deviation on the basis of the variance between tracks and a formal error (2 cm) added in quadrature. The 2-cm formal error is based on observed variations in effective reflector depth in the summer, when the reflector height should not change significantly. The uncertainty will thus be a result of not only a formal error but also a genuine spatial variability in snow depth over multiple tracks, which reflect off different parts of the ground. The formal error is based on the RMS of the residuals with respect to the model. In the future, we will extend this uncertainty assessment by including the effects of snow density uncertainty.

The GPS reflection footprint—expected to coincide with the first Fresnel zone (Hristov, 2000)—varies as a function of the height of the antenna above the ground and the satellite elevation angle and azimuth. First Fresnel zones for an antenna height of 3 m for a rising satellite are shown in Figure 1. The size of the ellipse is largest at 5° and gets progressively smaller and closer to the antenna as the satellite rises. By the time it reaches 30°, the Fresnel zone is only a few metres from the antenna. The snow depth estimates shown here come from a spatial footprint that is an average of the Fresnel zones between 5° and 20°. Although the 5° Fresnel zone implies a footprint ~80 m from the antenna, in practice the average GPS-IR signal comes from closer to the antenna (likely 25 m). For the western tracks, the average Fresnel zone is even closer to the antenna because the hill prohibits tracking below elevation angles of 7.5°.

Temporally, a GPS satellite takes ~40 min to rise from 5° to 20°. The GPS footprint is fairly stable over the year (moving tens of cm from east to west), but the measurement time changes by ~4 min/day. Thus, a track from satellite 12 observed at 18:00 UTC in January would appear at 10:00 UTC in May. Data collection from the GPS site during the winter was practically continuous. The only data gap occurred during the first 2 weeks of February, when the box containing the receiver was found open and the receiver was exposed to the elements.

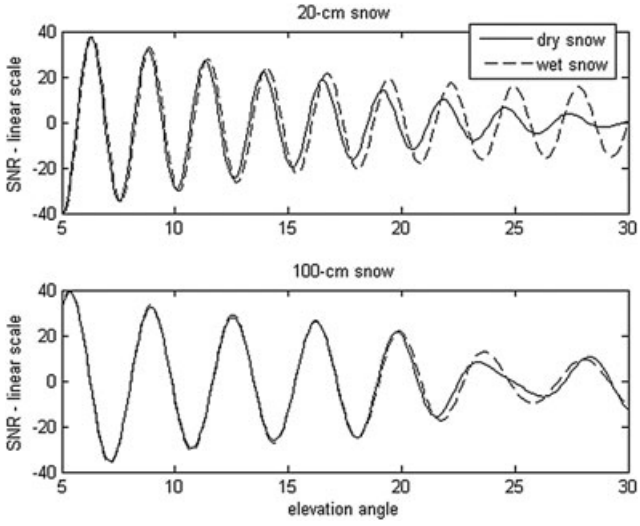

Figure 4. Modelled GPS SNR using permittivity derived from premelt snow density in April (solid line) and melt season snow density in May (dashed line) for both a shallow snowpack (top) and a deep snowpack (bottom). Based on the model of Zavorotny *et al.* (2010)

VERIFICATION DATA

Manual observations

Since 1982, the depth of the snowpack has been measured biweekly to monthly during the winter at the 88 points within the saddle grid at Niwot Ridge (Figure 1). Measurements during snowmelt were performed biweekly until all snow disappeared or until new snow began accumulating at the onset of the next winter. Measurements of snow depth were carried out to the nearest centimetre (Litaor *et al*., 2008). Here, we reported manual measurements of snow depths from a subset of the snow poles (poles 5, 6, 16 and 27). Pole 16 is located at the GPS antenna. Snow properties were analysed almost weekly at an index snow pit (usually beginning in January when snow depths exceed 0.50 m) near pole 6, following the protocol of Williams *et al.* (1999). Snow density was measured in vertical increments of 10 cm from the snow–atmosphere interface to the snow–ground interface, using a 1000-cm^3 stainless steel cutter and an

DOI: 10.1002/hyp

electronic scale (±2 g). The temperature of the snowpack was measured every 10 cm with 20-cm-long dial stem thermometers, calibrated to ±0.2 °C using a one-point calibration at 0 °C. Grain type, size and snowpack stratigraphy were also recorded. Depth-weighted values were then calculated for snowpack density, temperature and water equivalent.

Scanning laser rangefinder

The scanning laser rangefinder (Gutmann, 2010, 2011) makes snow depth measurements on a 25 × 35-m grid with a grid spacing just under 1 m (grid spacing varies slightly with snow depth). This system uses the SHM30 laser snow depth sensor manufactured by Jenoptik (http://www.jenoptik.com/en_40633_shm_30). The laser operates at 620–690 nm and is nominally accurate to 1–5 mm. The laser makes multiple measurements over a 0.1- to 6-s measurement interval and filters the results to remove noise caused by mid-air snowflakes. This laser was mounted on a d48 pan tilt unit made by Directed Perception (http://www.flir.com/mcs/products/ptu-d48/). The pan tilt unit has an angular step size of 0.006°. This system was mounted 19 m south west of the GPS, 5.5 m above the ground surface. It was anchored with guy wires at three points for stability and programmed to measure the grid of points with one measurement every 10 s.

The laser system has a precision of 1 mm on calm days and a sub-centimetre precision on windy days, but the absolute accuracy over longer times is uncertain because of small angular changes in the tower over time (Gutmann, 2010, 2011). The system measured a single grid point every 10 s and mapped the entire grid in just over 3 h. The laser was unable to make measurements farther than 10 m away in mid-day sunlight; thus, daytime measurements were limited. Daytime footprint average snow depths were corrected for these missing data by correlating the available mid-day measurements with the nighttime measurements from the night before and after each day. Problems with snow accretion on the lens prevented the laser rangefinder data set from being continuous during the accumulation period. We primarily compared the laser-mapped snow depth to the GPS for the period March 10 through June 6, a period in which the laser is recorded data nearly continuously and is expected to be accurate to ±5 cm. For the period October 29 to December 1 2009, the absolute value of the laser measurements is unknown, but the relative value is believed to be accurate to ±5 cm. During this period, the laser snow depth is tied to the GPS snow depth on November 10, 2009, at which point the snow was relatively dense and evenly distributed.

LIDAR

On May 21, 2010 (DOY 141), a LIDAR mission flew over the field site to collect snow-on information. The LIDAR data provide an independent method of verification of the GPS results. LIDAR data provide a surface elevation accurate to ~19 cm for grassy surfaces (Hodgson and Bresnahan, 2004). The data were collected, processed and archived by the National Center for Airborne Laser Mapping. The point measurements from the flight were averaged to make a digital elevation model (DEM) with a 1-m grid spacing. Because the laser pulse reflects from the surface of the snow (Deems *et al.*, 2006), this DEM represents the snow surface on this day. We obtained a map of snow depth for this day by subtracting a DEM generated from a snow-free LIDAR collection in 2006 by National Center for Airborne Laser Mapping.

RESULTS AND DISCUSSION

Meteorology

Winter 2009–2010 at Niwot ridge had below-average precipitation through February, with most of the accumulation for the season occurring in March, April and May. The site had a temperature range of −27 °C to +15 °C over the study period, with a typical diurnal temperature range of 5 to 10 °C on clear days. The average wind at 6 m height was 8 m/s and strong winds (>10 m/s) were out of the west (270 ± 30°) 80% of the time. A US Department of Agriculture, National Resources Conservation Service Snow Telemetry site below the ridge measured 551 mm of precipitation during this period, predominantly as snow; measurements are made with a single-alter shielded weighing all weather precipitation gauge (for a description, see Serreze *et al.*, 1999).

This precipitation, combined with the redistribution of snow by wind, resulted in peak snowpack depths that varied spatially from 0.7 to 1.7 m in April 2010 in the area around the GPS site. This is similar to the average peak snow accumulation of 1.0 to 1.6 m (from poles 6, 16 and 26; Litaor *et al.*, 2008). Most of this accumulation occurred in March–May. Although this is typical for the site, this season had a more pronounced seasonality than normal, with below average precipitation in October through February and above average precipitation for March, April and May. The late snow events in May prevented consistent snowmelt from starting until 21 May, although the snowpack became isothermal between 12 and 20 April. The spring was characterised by intermittent snowfalls and cold temperatures.

Manual measurements

Manual measurements at the GPS station (pole 16) record a peak snow depth of 1.3 m, whereas measurements 50 m southwest and south-southwest (poles 5 and 6, respectively) record a peak snow depth of 1.6 and 1.7 m (Figures 5 and 6, Table I). Measurements 50 m northeast (pole 27) only recorded a peak snow depth of 0.95 m. On DOY 141, the day of the LIDAR overflight, pole data interpolated between observations made 1 week prior and 1 week later suggest a snow depth of 1.35, 1.55, 1.1 and 0.82 m at poles 5, 6, 16 and 27, respectively (Table I).

Snow density ranged from 150 to 600 $kg \cdot m^{-3}$ for individual 1000-ml samples; snowpack average density was 390 $kg \cdot m^{-3}$ (±13) during the accumulation season (before

DOI: 10.1002/hyp

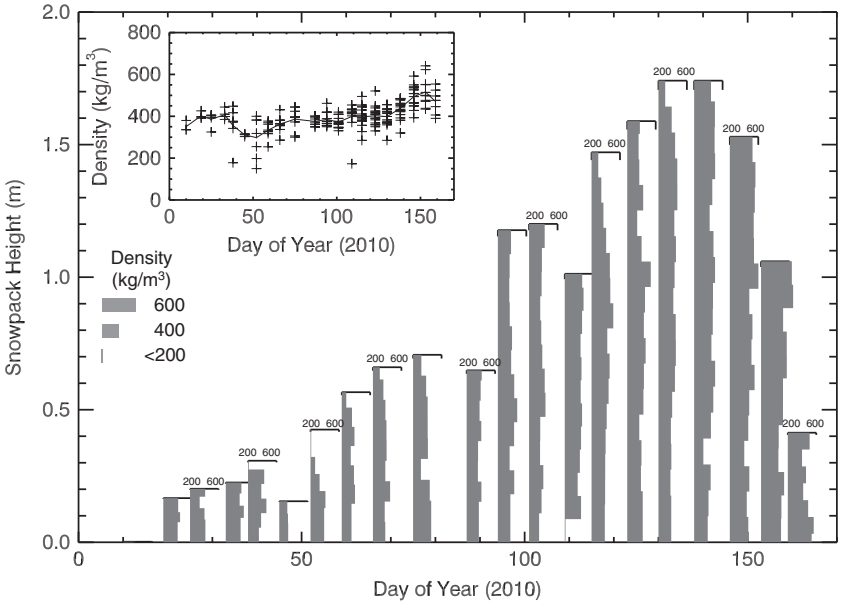

Figure 5. Measured snow pack depth and density over the 2010 snow season at pole 6

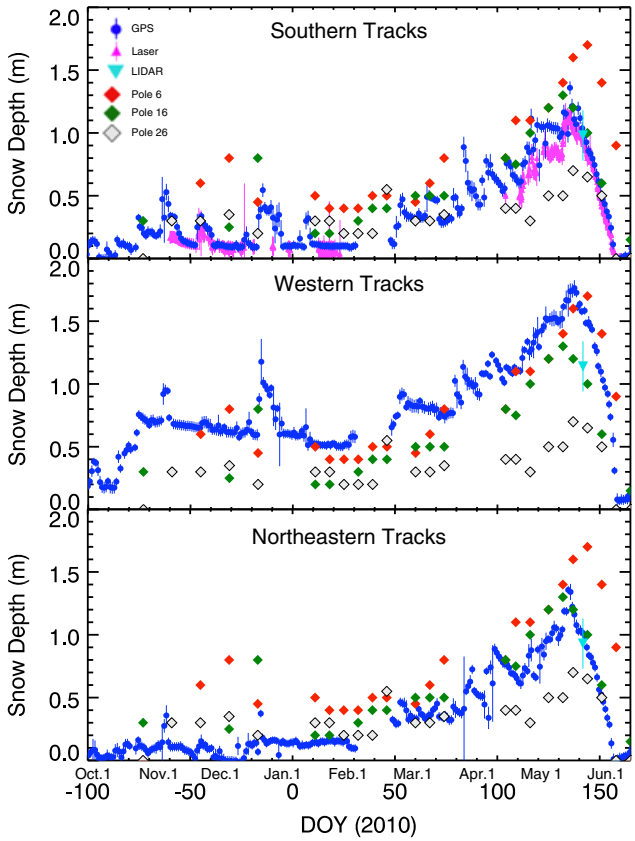

Figure 6. Snow depth measurements over time from manual measurements (diamonds pole 6, green; pole 16, white; and pole 26, red), GPS (blue dots) with error bars estimated from the variation between GPS satellites (see text), laser (magenta triangles with error bars from spatial variability) and LIDAR (cyan triangle), for the southern tracks (top), western tracks (middle) and northeastern tracks (bottom)

May 15, DOY 135) and 480 kg·m^{-3} (±34) during the melt season (after May 15) (see Figure 5). Density measurements show the extremely low densities (<200 kg·m^{-3}) at the surface immediately after snow events (e.g. DOY 40 and 52).

Table I. Observed maximum snow depth (m) and snow depth (m) on DOY 141 (date of LIDAR flight) for all measurement methods

Location		Peak	DOY 141
GPS	Southern	1.36	1.04
	Western	1.76	1.58
	Northeastern	1.36	1.02
Laser	Southern	1.15	0.93
LIDAR	Southern	–	1.03
	Western	–	1.15
	Northeastern	–	0.7
Manual pole	Pole 5 (South)	1.6	1.35
	Pole 6 (Southwest)	1.7	1.55
	Pole 16 (Center)	1.3	1.1
	Pole 27 (Northeast)	0.95	0.83

The variability of deeper layers over time is partially a function of the spatial variability of the snowpack because each measurement necessarily comes from a slightly different location. However, even with that variability, a spatially and temporally persistent low-density layer around 0.3 to 0.4 m above the ground is evident. This gives some indication of the stratigraphy within the snowpack.

Scanning laser measurements

Laser snow depth measurements recorded a peak snow depth of 1.15 m ± 0.06 m averaged over the GPS footprint (Figures 6 and 7, Table I). The standard deviation of snow depth recorded by the laser for a single grid snapshot in time averaged 7 cm over the entire season, and the range of snow depths was typically 45 cm. As indicated by the standard deviation, snow depth was relatively uniform throughout the GPS footprint mapped by the laser but varied substantially just outside this region, as evident in the airborne LIDAR data (Figure 8). At the time of the LIDAR overflight, the scanning laser measured a snow depth of 0.93 ± 0.05 m (Table I). The spatial variability

DOI: 10.1002/hyp

measured by the laser also changed over time. The standard deviation of snow depths varied from 4 to 9 cm during the accumulation period but remained steady at 5.5 cm through the later portion of the melt period.

LIDAR

The LIDAR data agree with manually measured snow depth across the entire 88-pole snow grid with an RMS error of 25 cm. Considering that the two measurements are not at exactly the same location, and that the spatial variability around the manual measurements is on the order of 10–15 cm, this error is considered a maximum. The bias between all of the manual observations and the nearly co-located LIDAR data is −3 cm (LIDAR less than manual). On DOY 141, the LIDAR data recorded a snow depth of 0.98 m ± 0.04 over the southern GPS tracks, 0.93 m ± 0.1 over the northeastern GPS tracks and 1.14 m ± 0.11 over the western GPS tracks (Figures 6–8, Table I). These estimates were derived over the average Fresnel zone, accounting for the size of the Fresnel zone on the day of the overflight by using the antenna height above the snow surface on this day.

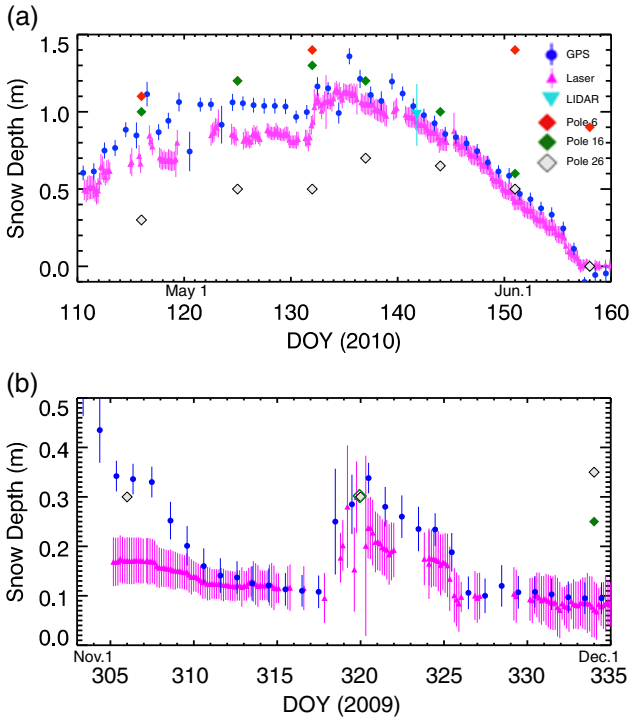

Figure 7. Snow depth measurements over time from the southern GPS tracks (symbols as in Figure 3) for the time (a) 10 April to 9 June 2010 and (b) 29 October to 1 December 2009; for the 2009 record, the laser depth was tied to the GPS on DOY 316

GPS data and comparison

GPS snow depth measurements ranged from zero to 1.76 m over a 300-day period (Figure 6). The western GPS tracks measured a deeper peak snow depth (1.76 m) than the southern (1.36 m) or the northeastern tracks (1.36 m). This compares favourably with nearby manual observations (1.3–1.7 m) and is slightly above the peak snow depth measured by the laser (1.15 m). The GPS also tracks the temporal evolution of the snowpack relative to both the laser and the manual observations (Figure 6). The GPS records a snow off date of DOY 156 over the southern and northeastern tracks, matching the laser observations and confirmed manually via a webcam. The GPS records a later snow off date, DOY 158, for the western tracks. Although the timing of this snow off date was harder to determine via webcam, it is clear from the webcam that the snow lasted longer to the west. On DOY 141, the day of the LIDAR flight, the GPS recorded a snow depth of 1.04 m on the southern tracks, 1.58 m on the western tracks and 1.02 m on the northeastern tracks.

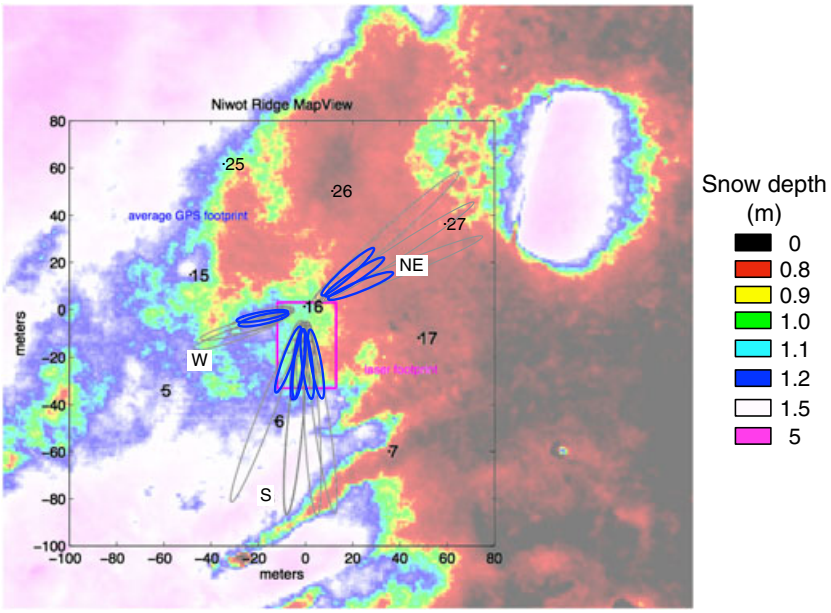

Figure 8. Spatial distribution of snow depth on DOY 141 as recorded by a LIDAR overflight. GPS Fresnel zones, laser footprint and manual pole locations as in Figure 1. Spatial distribution reflects topographical and wind controls. Snow dome on top right results from a snow fence at that location

DOI: 10.1002/hyp

The clearest comparison to the GPS comes from the scanning laser system rather than poles because it is measuring snow in a very similar location and over a larger area rather than at a point. During the melt period (DOY 135 on), the RMS difference between the GPS and the laser is 9 cm, with the laser typically recording 6 cm less than the GPS. These differences are comparable with the typical spatial variability recorded by the laser within the GPS footprint (5.5 cm). Over the entire period (DOY 110 on), the RMS difference between the GPS and the laser is 13 cm with a bias of 10 cm; this increase in error corresponds with the increase in variability recorded by the laser (~8–10 cm) during this time. The bias between the laser and the GPS may be because the GPS is sensitive to a region further south than the laser, and manual observations (poles 5 and 6) from south of the GPS suggest the snow is deeper in this region. This assessment of spatial variation is further validated by the LIDAR data on DOY 141 (Figure 8). The LIDAR data show that snow depth increases from a mean of 0.92 m in the region the laser is measuring (0–30 m from the GPS) to 1.3 m in the region 30–50 m from the GPS (Figure 9). However, although the average Fresnel zone for a 3-m antenna may encompass the region >30 m south of the antenna, once a meter of snow is on the ground (making the antenna height 2 m), the Fresnel zone will shrink so that the GPS is averaging over a region approximately 3–20 m away from the antenna.

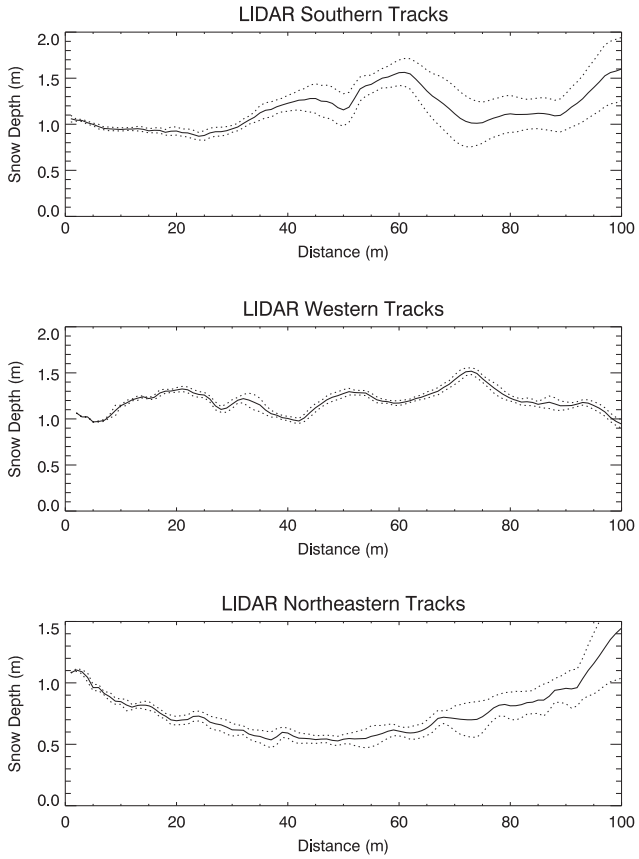

Figure 9. Snow depth profiles from LIDAR data for three GPS regions, southern tracks (top), western tracks (middle) and northeastern tracks (bottom); in all cases, the GPS is at 0 m on the *x*-axis. Mean (solid line) is plotted with one standard deviation above and below (dotted line)

The temporal evolution of the laser and the GPS shows that, before DOY 130, the laser measures substantially less snow on the ground than the GPS does. This could be due to several factors. First, the density of the snow in this period is lower, and we may not be accurately including this effect, especially because the top 10 cm is typically less dense than the snowpack average (Figure 5). However, these small changes in snow density should not substantially alter the GPS depth measurements (Figure 4). Second, the pole the laser is mounted on could have shifted in the early snow conditions, thus making its measurement less reliable in this period (Gutmann, 2011). Third, earlier in the season, the GPS will be sensitive to a region further south because there is less snow on the ground. Fourth, the spatial variability observed during the melt season is typically less pronounced compared with the accumulation season, increasing the disparity between the real snow depth in the laser and GPS footprints (Williams and Melack, 1991; Williams *et al.*, 2001).

During the accumulation period, the GPS also clearly records individual snowstorms following a pattern that would be expected for this location (Figure 7b). There is a sharp increase in snow depth during the storm, followed by a steady decrease in snow depth as the fresh, poorly consolidated snow is both compacted and scoured by the wind. This same pattern was recorded by the scanning laser system for the storms in which it was able to make continuous measurements. However, the laser and the GPS differ on the amount of snow depth variation; this could be a result of two separate factors. First, we again note that the GPS and the laser are viewing different areas, and it is possible that the region further south, which the GPS may be sensitive to, received substantially more snow deposition than the region in which the laser is sensitive. This would not be due to spatial variation in actual snowfall but rather to spatial variation in wind loading and scouring.

Second, fresh snow will have a much lower density (~100–200 $kg \cdot m^{-3}$) than older consolidated snowpack (300–500 $kg \cdot m^{-3}$), as a result, it will have a different effect on the GPS signal (Figure 4). However, theoretically, the main effect of the lower snow density is a decrease in the amplitude of the SNR oscillations at high elevation angles, with a larger effect when the snowpack is shallower. For shallow snowpacks, the GPS signal that penetrates the snowpack will reflect off the ground and be received by the GPS antenna. This second reflection is combined with the effect of the primary (top of snow) reflection and may mute the signal. In deeper snowpacks, the ground reflection will be absorbed by the snow along the signal path. In addition, this effect only appears at higher elevation angles (>20°) because at low elevation angles, the path length through the snow is greater leading to greater absorption and the surface reflectance is higher.

In comparison to the manual observations, the GPS records a shallower snowpack than poles 5, 6 and 16 on the southern track. Because the GPS observations are in line with the scanning laser and the LIDAR overflight, we suspect that this represents the spatial variability in the field. In other words, the poles are located at sites that get

DOI: 10.1002/hyp

slightly more snow than the GPS footprint. This hypothesis fits with the GPS data from the western tracks and the LIDAR data. The western GPS data show a deeper peak snowpack (1.76 m) similar to pole 6 peak snowpack (1.7 m) at the same time. Similarly, the LIDAR data from DOY 141 record a snow depth of 0.98 m on the southern track and 1.14 m on the western track. As noted earlier, the manual observations, interpolated from observations 1 week before and 1 week after the LIDAR overflight, suggest a snowpack of 1.55 m at pole 6 and 1.1 m at pole 16, illustrating the difference between the manual point observations and the field average snowpack.

One location for which the GPS performance is not well understood is over the western tracks (Figure 6). The scanning laser does not cover these tracks, so the only comparisons that are possible are to the manual observations and the LIDAR overflight. On the western tracks, the GPS and the pole 6 data have similar peak snow depths, but the LIDAR data suggest that the snow the GPS is actually sensing is not as deep. On DOY 141, the LIDAR data record a snow depth of $1.14\,\text{m} \pm 0.1\,\text{m}$, whereas the GPS records a snow depth of 1.58 m. Indeed, the deepest snow depth in the LIDAR data for the western track is only 1.45 m. Although the LIDAR may have errors as high as 0.3 m, our comparison to the manual observations suggest that it is less than that on average ($\text{RMS} = 0.25\,\text{m}$, $\text{bias} = -0.03\,\text{m}$). This region may partially be affected by steeper topographic slopes and we will investigate this more in the future.

CONCLUSIONS

Snow depth variations associated with accumulation and ablation were measured using GPS-IR over an entire winter season in an environmentally and topographically challenging site, then validated against terrestrial and airborne laser mapping as well as manual snow surveys. We have shown that GPS-IR can accurately measure snow depth in a cold, dry alpine environment within 9 to 13 cm. When one considers the differences between the locations of the GPS measurement and the verification measurement, the GPS may actually be more accurate than that. Snow depth can be measured in both accumulation and melt periods, despite variations in snow density and water content. However, snow depth increases during snowfall events may be overestimated (5–10 cm bias). A model that incorporates variability in snowpack density as well as more complex topography and spatial heterogeneity in snow depth and roughness may improve on the current results.

Despite the success of most of these measurements, the western GPS tracks do not match the limited observations available as closely as the southern or northeastern tracks do. This suggests that more work needs to be done to understand the spatial footprint of the GPS and the role of surrounding topography. In particular, large-scale changes in reflector height, slope and aspect as well as the spatial distribution of surface roughness may affect the footprint, and this will be the subject of future research. Additional snow depth data will be collected in these regions in the future to aid interpretation of the signal.

In addition to providing a data set that generally matches both the laser and manual observations to within errors, the GPS provides a more continuous set of measurements than either the laser or the manual observations. Manual observations require a human in the field and thus were limited to biweekly observations at individual poles during reasonable weather conditions. Laser measurements were hampered by ice accumulation on the lens and background sunlight, both of which limited the periods in which the laser was able to measure the snow surface. Furthermore, a laser is unable to provide snow density estimates, which is theoretically possible with GPS-IR (Jacobson, 2010).

In future work, we will further develop GPS-IR in several aspects. In forward modelling, we are extending GPS-IR to support not only flat surfaces—horizontal as in Larson *et al*. (2010) or tilted as in the present work—but also those affected by large-scale undulations as well as small-scale roughness. This will alleviate the topographical requirements for a feasible GPS-IR site. In addition, a statistical inverse model is under testing. It may address the demands for SWE estimates and some of the discrepancies surrounding individual snow events seen in this study. Eventually, GPS-IR should be demonstrated over a greater number of stations, thus delivering on the promise of leveraging hundreds of existing ground-based GPS stations as a complement to existing snow monitoring networks such as the Service Snow Telemetry.

ACKNOWLEDGEMENTS

KL and FGNs contributions were supported by NSF EAR 0948957, a CU interdisciplinary seed grant, and a grant from the CU engineering college. FGN acknowledges funding provided by Fulbright/Capes. The NSF-funded NWT LTER project provided field and logistical support as well as the contributions of MWW. The receiver used at Niwot Ridge was leant to the project by Trimble Navigation. UNAVCO provided engineering and archiving support. The National Center for Atmospheric Research is sponsored by the National Science Foundation. EDG was supported by a postdoctoral programme of the Advanced Study Program at the National Center for Atmospheric Research. LIDAR information was provided by the NSF-funded Boulder Creek Critical Zones Observatory. The authors thank two anonymous reviewers who have made this a better article.

REFERENCES

Armstrong RL, Brun E (eds.). 2008. *Snow and Climate—Physical Processes, Surface Energy Exchange and Modeling*. Cambridge University Press: Cambridge; 222.

Barnett TP, Adam JC, Lettenmaier DP. 2005. Potential impacts of a warming climate on water availability in snow-dominated regions. *Nature* **438**(17): 303–309.

Caine N. 1996. Streamflow patterns in the alpine environment of North Boulder Creek, Colorado Front Range. *Zeitschrift für Geomorphologie* **104**: 27–42.

Deems JS, Fassnacht SR, Elder KJ. 2006. Fractal Distribution of Snow Depth from LIDAR Data. *Journal of Hydrometeorology* **7**: 285–297.

Desilets D, Zreda M, Ferré T. 2010. Nature's neutron probe: Land-surface hydrology at an elusive scale with cosmic rays. *Water Resources Research* **46**: W11505. DOI: 10.1029/2009WR008726

Eisen O, Frezzotti M, Genthon C, Isaksson E, Magand O, van den Broeke MR, Dixon DA, Ekaykin A, Holmlund P, Kameda T, Karlöf L, Kaspari S, Lipenkov VY, Oerter H, Takahashi S, Vaughan DG. 2008. Ground-based measurements of spatial and temporal variability of snow accumulation in East Antarctica. *Reviews of Geophysics* **46**: RG2001. DOI: 10.1029/2006RG000218

Erickson T, Williams MW, Winstral A. 2005. Persistence of topographic controls on the spatial distribution of snow depth in rugged mountain terrain, Colorado, USA. *Water Resources Research* **41**(4): W04014. DOI: 10.1029/2003WR002973

ESA. 2008. CoReH2o—COld REgions Hydrology high-resolution Observatory. European Space Agency SP-1313/3 Candidate Earth Explorer Core Missions—Report for Assessment.

Fontana RD, Cheung W, Novak PM, Stansell TA. 2001. The New L2 Civil Signal. in *Proceedings of the 14th International Technical Meeting of the Satellite Division of the Institute of Navigation ION GPS*, September 11–14, 617–631.

Gutmann ED. 2010. Continuous alpine snow depth mapping by laser rangefinder through a winter season. Abstract C33C-0524 presented at 2010 Fall Meeting, AGU, San Francisco, Calif., 13–17 Dec.

Gutmann ED. 2011. Continuous snow depth mapping using a scanning laser rangefinder, *in prep*.

Hardy J, Davis R, Koh Y, Cline D, Elder K, Armstrong R, Marshall HP, Painter T, Saint-Martin GC, DeRoo R, Sarabandi K, Graf T, Koike T, McDonald K. 2008. NASA Cold Land Processes Experiment (CLPX 2002/03): Local Scale Observation Site. *Journal of Hydrometeorology* **9**: 1434–1442.

Hodgson ME, Bresnahan P. 2004. Accuracy of Airborne LIDAR-Derived Elevation: Empirical Assessment and Error Budget. *Photogrammetric Engineering and Remote Sensing* **70**(3): 331–339.

Hristov HD. 2000. Fresnel zones in wireless links, zone plate lenses and antennas, Artech House, ISBN 9780890068496, 323.

IGOS. 2007. *Integrated Global Observing Strategy Cryosphere Theme Report—For the Monitoring of our Environment from Space and from Earth*. World Meteorological Organization: Geneva. WMO/TD-No. 1405, 100.

Jacobson MD. 2008. Dielectric-Covered Ground Reflectors in GPS Multipath Reception — Theory and Measurement. *IEEE Geoscience and Remote Sensing Letters* **5**(3). DOI: 10.1109/LGRS.2008.917130.

Jacobson MD. 2010. Inferring Snow Water Equivalent for a Snow-Covered Ground Reflector Using GPS Multipath Signals. *Remote Sensing* **2**: 2426–2441. DOI: 10.3390/rs2102426

Larson KM, Small EE, Gutmann E, Bilich A, Braun J, Zavorotny V. 2008. Use of GPS receivers as a soil moisture network for water cycle studies. *Geophysical Research Letters* **35**: L24405. DOI: 10.1029/2008GL036013

Larson KM, Gutmann E, Zavorotny V, Braun J, Williams M, Nievinski FG. 2009. Can we measure snow depth with GPS receivers? *Geophysical Research Letters* **36**: L17502. DOI: 10.1029/2009GL039430

Larson KM, Braun J, Small EE, Zavorotny V, Gutmann E, Bilich A. 2010. GPS Multipath and Its Relation to Near-Surface Soil Moisture Content. *IEEE Journal of Selected Topics in Applied Earth Observations and Remote Sensing* **3**: 91–99. DOI: 10.1109/JSTARS.2009.2033612

Litaor MI, Williams MW, Seastedt T. 2008. Topographic controls on snow distribution, soil moisture, and species diversity of herbaceous alpine vegetation, Niwot Ridge, Colorado. *Journal of Geophysical Research: Biogeosciences* **113**: G02008. DOI: 10.1029/2007JG000419

Mätzler C. 1996. Microwave permittivity of dry snow. *IEEE Transactions on Geoscience and Remote Sensing* **34**(2): 573.

Parry ML, Canziani OF, Palutikof JP, Adger N, Aggarwal P, *et al*. 2007. Technical summary. In *Climate Change 2007: Impacts, Adaptation and Vulnerability, Contribution of Working Group II to the Fourth Assessment Report of the Intergovernmental Panel on Climate Change*, Parry ML, Canziani OF, Palutikof JP, van der Linden PJ, Hanson CE (eds). Cambridge Univ. Press: Cambridge, UK; 23–78.

Prokop A. 2008. Assessing the applicability of terrestrial laser scanning for spatial snow depth measurements. *Cold Regions Science and Technology* **54**(3): 155–163.

Scott D, Dawson J, Jones B. 2008. Climate change vulnerability of the US Northeast winter recreation– tourism sector. *Mitigation and Adaptation Strategies for Global Change* **13**: 577–596. DOI: 10.1007/s11027-007-9136-z

Serreze MC, Clark MP, Armstrong RL, McGinnis DA, Pulwarty RS. 1999. Characteristics of the western United States snowpack from snowpack telemetry (SNOTEL) data. *Water Resources Research* **35**(7): 2145–2160.

Small EE, Larson KM, Braun JJ. 2010. Sensing Vegetation Growth With Reflected GPS Signals. *Geophysical Research Letters* **37**: L12401. DOI: 10.1029/2010GL042951

Williams MW, Melack JM. 1991. Solute chemistry of snowmelt and runoff in an alpine basin, Sierra Nevada. *Water Resources Research* **27**: 1563–1574.

Williams MW, Losleben M, Caine N, Greenland D. 1996. Changes in climate and hydrochemical responses in a high-elevation catchment, Rocky Mountains. *Limnology and Oceanography* **41**(5): 939–946.

Williams MW, Cline D, Hartmann M, Bardsley T. 1999. Data for snowmelt model development, calibration, and verification at an alpine site, Colorado Front Range. *Water Resources Research* **35**(10): 3205–3209.

Williams MW, Hood E, Caine N. 2001. The role of organic nitrogen in the nitrogen cycle of a high-elevation catchment, Colorado Front Range, USA. *Water Resources Research* **37**(10): 2569–2582.

Zavorotny V, Larson KM, Braun J, Small EE, Gutmann E, Bilich A. 2010. A physical model of GPS multipath caused by land reflections: toward bare soil moisture retrievals. *IEEE J-STARS* **3**(1): 100–110. DOI: 10.1109/JSTARS.2009.2033608